

CHEMISTRY

AN **ASIAN** JOURNAL

www.chemasianj.org

Accepted Article

Title: Nature of Bonding in Bowl-Like B₃₆ Cluster Revisited. Concentric (6 π Plus 18 π) Double Aromaticity and Reason for the Preference of Hexagonal Hole in Central Location

Authors: Hua-Jin Zhai, Rui Li, Xue-Rui You, and Kang Wang

This manuscript has been accepted after peer review and appears as an Accepted Article online prior to editing, proofing, and formal publication of the final Version of Record (VoR). This work is currently citable by using the Digital Object Identifier (DOI) given below. The VoR will be published online in Early View as soon as possible and may be different to this Accepted Article as a result of editing. Readers should obtain the VoR from the journal website shown below when it is published to ensure accuracy of information. The authors are responsible for the content of this Accepted Article.

To be cited as: *Chem. Asian J.* 10.1002/asia.201800174

Link to VoR: <http://dx.doi.org/10.1002/asia.201800174>

A Journal of



A sister journal of *Angewandte Chemie*
and *Chemistry – A European Journal*

WILEY-VCH

**Nature of Bonding in Bowl-Like B₃₆ Cluster Revisited.
Concentric (6 π Plus 18 π) Double Aromaticity and Reason for
the Preference of Hexagonal Hole in Central Location**

Rui Li, Xue-Rui You, Kang Wang, and Hua-Jin Zhai*


[*] R. Li, X.-R. You, K. Wang, Prof. Dr. H.-J. Zhai

Nanocluster Laboratory

Institute of Molecular Science

Shanxi University, Taiyuan 030006 (China)

E-mail: hj.zhai@sxu.edu.cn

 Supporting information and the ORCID identification number(s) for this article can be found under <https://doi.org/10.1002/asia.xxxxxxxx>.

Abstract

Bowl-shaped C_{6v} B_{36} cluster with a central hexagon hole is considered an ideal molecular model for low-dimensional boron-based nanosystems. Owing to electron-deficiency of boron, chemical bonding in B_{36} cluster is intriguing and complicated and has remained elusive despite a couple of papers in literature. Herein we shall offer an in-depth bonding analysis via canonical molecular orbitals (CMOs) and adaptive natural density partitioning (AdNDP), further aided with natural bond orbital (NBO) analysis and orbital composition calculations. The concerted computational data establish the idea of concentric double π aromaticity for B_{36} cluster, with inner 6π and outer 18π electron-counting, which both conform to the $(4n + 2)$ Hückel rule. The updated bonding picture differs from existing knowledge of the system. A refined bonding model is also proposed for coronene, of which B_{36} cluster is an inorganic analogue. It is further shown that concentric double π aromaticity in B_{36} cluster is retained and spatially fixed, irrespective of the migration of hexagonal hole; the latter process varies the system energetically. Hexagonal hole is found to be a destabilization factor for σ/π CMOs. The central hexagon hole affects substantially fewer CMOs, thus making bowl-shaped C_{6v} B_{36} cluster the global minimum.

Keywords: boron clusters, hexagonal hole, concentric double π aromaticity, canonical molecular orbitals (CMOs), adaptive natural density partitioning (AdNDP).

1. Introduction

Elemental boron clusters^[1–22] possess highly unusual structural and bonding properties owing to the intrinsic electron-deficiency of boron. Systematic experimental and computational studies in the past 30 years have uncovered an unprecedented zoo of planar or quasi-planar (2D) boron clusters, up to some 40 atoms for the anions.^[9,21] Among notable 2D boron species is a B₃₆ cluster,^[17,18] which is bowl-shaped and triangularly close-packing with C_{6v} symmetry, featuring a hexagonal hole in the center as “defect”. It is widely considered as a molecular model for low-dimensional boron nanomaterials, such as boron α -sheets,^[23–25] borospherenes,^[20,21] and in particular borophenes,^[26–29] in which close-packing boron ribbons or sheets and hexagonal holes prevail. Given the importance of B₃₆ cluster in the field, its structural, electronic, and bonding properties require in-depth analyses and understanding.

However, chemical bonding in boron clusters^[9,30] of such a size as B₃₆ turns out to be rather challenging for theoretical chemistry. With over 100 valence electrons, detailed and thorough analyses of canonical molecular orbitals (CMOs) can be a heroic effort if not impossible. Newly developed tools such as adaptive natural density partitioning (AdNDP)^[31] are applicable, but the program is user-adapted and the interpretation of its output requires expertise. Consequently, we believe the exact nature of bonding in B₃₆ cluster has remained elusive, despite a couple of prior computational works.^[17–19] Interestingly, Liu et al.^[19] recently raised a question with regard to bonding and energetics in B₃₆ cluster: why the hexagonal hole prefers to be located at the central position? To our understanding, this fundamental question is still open.

In this contribution, we choose to address two critical open issues on bowl-like B₃₆ cluster as outlined above. What is the nature of bonding in B₃₆ cluster? Why is the hexagonal hole situated in the bowl center in B₃₆ cluster? To this end, we have performed in-depth bonding analyses via CMOs and AdNDP, which are further aided by natural bond orbital (NBO)^[32] analysis and orbital composition calculations.^[33] Our computational data leads to a bonding picture of concentric double π aromaticity, with the 6π and 18π electron-counting for inner and outer subsystems, respectively, which both follow the $(4n + 2)$ Hückel rule. We briefly reason why the

Hückel rule applies for bowl-like B_{36} cluster, although it is not a monocyclic system. We also uncover the reason behind the central position of hexagonal hole in B_{36} cluster. The hexagonal hole turns out to be a destabilization factor for CMOs that covers it. While electron clouds associated to double π aromaticity are maintained and spatially fixed during the migration of hexagonal hole in a series of B_{36} isomers, the central hexagonal hole manages to affect markedly fewer CMOs (that is, to minimize the destabilization due to hexagonal hole). As a consequence, bowl-shaped C_{6v} B_{36} cluster with a central hexagon hole becomes global minimum (GM) of the system.

2. Methods

Isomeric structures **I**, **II**, and **III** of B_{36} cluster were constructed based on literature,^[17–19] followed by full re-optimizations using density-functional theory (DFT) at the PBE0 level^[34] with the 6-311+G(d) basis set.^[35] Vibrational frequencies were calculated at the same level to ensure that all three isomers are true minima on their potential energy surface. Chemical bonding in the B_{36} isomers and their polycyclic aromatic hydrocarbon (PAH) analogue, coronene ($C_{24}H_{12}$), were elucidated using the CMO analysis and AdNDP, which deals with all valence electrons, both σ and π . Since AdNDP analysis is not sensitive to the level of theory or basis sets used, we chose to carry out calculations at PBE0/6-31G level, using the AdNDP program.^[31]

The NBO analysis^[32] were performed to obtain natural atomic charges and Wiberg bond indices (WBIs), whereas natural atomic orbital (NAO) calculations^[33] were done for the analysis of orbital compositions. All electronic structure calculations were accomplished using the Gaussian 09 software package.^[36] Orbital compositions were calculated using the Multiwfn^[33] package. Visualization of the AdNDP results was realized using Molekel.^[37] Cluster structures and their CMOs were visualized using GaussView 5.0.9.^[38]

3. Results and Discussion

3.1. Structures and energetics of isomers **I**, **II**, and **III** of B_{36} cluster

Three isomers of B_{36} cluster (**I**, **II**, and **III**), as optimized at PBE0 level, are illustrated in Figure 1. Structure **I** has a perfect bowl shape with C_{6v} symmetry. For the sake of clarity, we define herein that the cluster is composed of three concentric B rings, labeled from core to periphery as the *first* (B_6), *second* (B_{12}), and *third* (B_{18}) ring, respectively. We further define that the first and second B rings make an *inner* boron double ring (BDR) ribbon, whereas the second and third B rings form an *outer* BDR ribbon. The inner BDR ribbon has 18 atoms, as compared to 30 atoms for the outer ribbon. As will be shown below, essential bonding elements in isomers **I–III** are all clouded on the BDR ribbons, rather than on specific B rings.

Structure **I** is the GM of B_{36} cluster,^[17–19] featuring ideal inner and outer BDR ribbons. It also has a characteristic hexagonal hole^[20,21,23–28] at the center. Six apex B atoms in the third B ring are tricoordinated and the remaining 12 edge B atoms tetracoordinated. For comparison, the 6 and 12 B atoms in the first and second B rings have penta- and hexacoordination, respectively. The different coordination environments hint that each kind of B sites may participate in chemical bonding in distinct ways (*vide infra*).

Overall, GM **I** is about 40 and 61 kcal mol⁻¹ below isomers **II** and **III**, respectively (Figure 1). These values are virtually identical to those of Liu et al.^[19] at PBE0/def2-TZVP level. Structures **I–III** differ only in the position of hexagonal hole: at the center of first B ring in **I**, on the first B ring in **II**, and on the second B ring in **III**. As a result, the inner BDR ribbon in **II** is not closed due to a defect, and yet it also has a filled and imperfect “disk” center. Note that similar pentacoordinate boron motifs were previously observed in B_{24}^- and B_{25}^- clusters.^[39,40] In contrast, neither the inner nor outer BDR ribbon in **III** is closed due to the defect, although it has a perfect hexacoordinate B_7 disk at the center.

With the moving of hexagonal hole from bowl center out, the energetics of B_{36} cluster elevates gradually and monotonously, demonstrating the preference of hexagonal hole in the central location as revealed initially by Liu et al.^[19] This observation is intriguing and should be rationalized on the basis of in-depth bonding analyses. Indeed, a prerequisite is that the bonding analyses need to be complete and correct, which are not a trivial task despite numerous prior

attempts.^[17–19] This is understandable considering the size of the system, as well as the nature of electron-deficiency and multifold (σ and π) aromaticity in planar boron clusters.^[9,41]

3.2. Bonding in B₃₆ cluster revisited: Concentric inner 6 π plus outer 18 π double aromaticity

We focus on the bonding in bowl-like B₃₆ (**I**) cluster, whose complete set of π CMOs are shown in Figure 2a. As a starting point for discussion, for a polygonal n -membered molecular system, each specific atomic orbital (AO) can in principle combine into a set of n CMOs, which have 0, 1, 2, ..., nodal planes from bottom up.^[42–44] When all n CMOs are fully occupied, they can be transformed to localized Lewis elements, either two-center two-electron (2c-2e) bonds or lone-pairs. Otherwise, they form a delocalized system, rendering aromaticity or antiaromaticity according to the Hückel electron-counting rules.

Bowl-like B₃₆ (**I**) cluster has a total of 108 valence electrons. To form a primitive molecular skeleton, the first and third B rings use 12 and 36 electrons, respectively, for localized 2c-2e σ bonds,^[45] which has been established to be routine for planar boron clusters.^[9,41] Indeed, a set of six σ CMOs with 0, 1 (degenerate), 2 (degenerate), and 3 nodal planes are readily identified for the first B ring. Similarly, along the third B ring a full set of eighteen σ CMOs can be found.^[46] AdNDP analyses recover these six plus eighteen σ bonds, which are presented as 2c-2e/3c-2e σ bonds in Figure 3a.^[18] See note^[45] for clarification of the 2c-2e versus 3c-2e issue.

Other than those mentioned above, 18 σ CMOs as depicted in the Supporting Information (Figure S1) are located on the inner and outer BDR ribbons. The 12 CMOs in Figure S1b are primarily clouded on the outer ribbon (by 72%–94% based on orbital component analysis), with the deeper six also having secondary contributions from the inner ribbon. These CMOs strictly follow the building principle with from 0 up to 6 nodal planes, which owing to the C_{6v} symmetry can be effectively “islanded” as 12 σ bonds (upon destructive/constructive combination with the six CMOs in Figure S1a). The most reasonable scheme is twelve rhombic 4c-2e σ bonds along the outer BDR ribbon (Figure 3a). Here each apex atom in the third B ring is associated to two 4c-2e σ bonds. It is stressed that this scheme is an approximation, because σ delocalization is

known to be crucial in boron clusters.^[47–49] People would even argue that the most important contribution to electron delocalization comes from σ electrons. However, the occupation numbers (ONs; 1.89–1.95 |e|) are close to ideal. Likewise, six CMOs in Figure S1a have 54–70% contributions from inner BDR ribbon. They can combine constructively/destructively with bottom six CMOs in Figure S1b to obtain a set of σ bonds on the inner ribbon, which have from 0 up to 3 nodal planes and correspond to six 4c-2e σ bonds (see AdNDP data in Figure 3a).

In short, we have reasoned above in full detail, via CMO analyses, that cluster **I** has six and eighteen 2c-2e/3c-2e σ bonds on the first and third B rings, respectively, as well as six and twelve 4c-2e island σ bonds on the inner and outer BDR ribbons, respectively. These σ bonds cover the whole cluster surface almost uniformly, collectively consuming 42 pairs of electrons. The σ framework^[17,18] is elegantly summarized in the AdNDP scheme (Figure 3a, top row).

The π framework seems to be simpler and relatively straightforward in terms of CMOs (Figure 2a); see also Figure S2 for isomer **II** and Figure 4 for isomer **III**. However, it turns out to be challenging to reach an essential bonding picture from the π CMOs for a number of reasons. First, it is fundamental and open whether the $(4n + 2)$ and $4n$ Hückel rules apply for polycyclic clusters such as **I–III**. Second, if they do, how? Third, is a system with twelve π CMOs (that is, 24π electrons) in line with the $4n$ Hückel rule? Is it aromatic or antiaromatic? Fourth, how does the user-adapted AdNDP program^[31] help in elucidating such a complex π bonding system?

The π CMOs (Figure 2a) are composed of B $2p_z$ AOs, following the building principle as mentioned above for σ framework. These can be divided spatially into two subsets: three π CMOs for the inner BDR ribbon (HOMO–1, HOMO–1', and HOMO–5; with secondary components from the third ring by 48–49%) and the remaining nine CMOs for the outer ribbon. Of course, there are mixing between inner and outer ribbons for certain CMOs. Indeed, bottom three CMOs for outer ribbon (HOMO–17, HOMO–17', and HOMO–18) contain 21–29% from the first ring; these combine constructively/destructively with those of inner ribbon to fully recover three π CMOs for inner BDR ribbon. Their corresponding destructive/constructive combination leads to three “purified” π CMOs clouded on the outer ribbon, which along with six

higher π CMOs (HOMO, HOMO', HOMO-3, HOMO-6, HOMO-10, and HOMO-10') form an extensive series with from 0 up to 4 nodal planes, including four pairs of degenerate CMOs. Note that for π bonds, the intrinsic nodal plane associated p_z AOs is not counted, as routine. The inner and outer π subsystems are perfectly recovered in AdNDP analysis (Figure 3a).

The π system in inner BDR ribbon (Figure 3a, second row) is exactly analogous to the π sextet in benzene, except that the former is clouded on a BDR ribbon instead of a single B ring. The reason for this is that B is electron-deficient with respect to C, so that boron double rings collectively function as a single C ring.^[50-52] Such a π sextet cannot be localized even in a single C_6 ring in benzene. In B_{36} (**I**), the inner π sextet is 18-center in nature and intrinsically delocalized, which renders π aromaticity for the cluster according to the Hückel rule.

For the outer BDR ribbon, a π subsystem with nine CMOs is identified (Figure 2a, second and third rows). Their corresponding AdNDP bonds are shown in Figure 3a, which are slightly modified with respect to CMOs and become strictly 30c-2e in nature (rather than global). These π bonds are located on the outer ribbon, following a regular pattern of from 0 up to 4 nodal planes, which is a genuine and complete series and *cannot be arbitrarily divided, segmented, islanded, or localized*. With this understanding, the 18π electron-counting again conforms to the $(4n + 2)$ Hückel rule, thus rendering double π aromaticity for the cluster. Therefore, our CMO analyses firmly establish a concentric, doubly π aromatic system, with electron-counting of 6π for the inner BDR ribbon and 18π for the outer. AdNDP data fully reproduce this bonding picture (Figure 5a), which differs fundamentally from prior knowledge of the system.^[17,18] Specifically, Chen et al.^[18] stated an inner π sextet as well as an outer π sextet. Piazza et al.^[17] reached a “global” 12π electron system without the spatial distinction between inner and outer BDR ribbons, whose electron-counting presumably satisfies the $4n$ Hückel rule. The 12π system^[17] exhibits 0, 1, 3, and 4 nodal planes in AdNDP, which is not a complete series of bonds that follow the construction principle. In particular, only one AdNDP bond has 3 nodal planes, in contrast to two AdNDP bonds with 4 nodal planes.

We shall add a few comments here: (i) B_{36} (**I**) is a polycyclic cluster rather than monocyclic. Nonetheless, once it is viewed as a concentric cluster with inner and outer BDR ribbons and consists of spatially separated double π subsystems, each BDR ribbon (and π subsystem) is equivalent to a monocyclic system, because a BDR ribbon is equivalent to a C single chain.^[50–52] Thus the $(4n + 2)$ and $4n$ Hückel rules, which many people believe to be valid for monocyclic systems only, apply for bowl-shaped B_{36} (**I**) cluster. (ii) B_{36} (**I**) cluster is doubly π aromatic, despite the fact that it has a total of 24π electrons. This π framework needs to be subdivided into 6π versus 18π subsystems, because they are spatially independent from each other and should be counted separately. (iii) AdNDP analysis is user-adapted and the data should be examined with caution. In fact, for the outer BDR ribbon in B_{36} (**I**) cluster, a prior analysis^[18] generated six “island” 4c-2e π bonds on apex sites as well as three global 36c-2e π bonds (that is, the outer π “sextet”), which differ from the scheme in Figure 5a. The reason is that AdNDP automatically, and indeed arbitrarily, segments the nine π CMOs (Figure 2a, second and third rows) into two parts, so that the lower six are islanded as six 4c-2e π bonds, with higher-energy three (HOMO, HOMO', and HOMO–3) remaining delocalized because it is simply not possible to localize those! Such a scheme is actually “hybrid” and arbitrary. It is stressed that the “ π sextet” is abnormal with the lowest-energy bond having as many as 3 nodal planes. As stated earlier, such a bond should normally be completely delocalized and completely bonding! (iv) We alert that similar, unreasonable AdNDP schemes are found in literature for other clusters as well, which motivated us to undertake the present study. We believe our analysis will benefit the field.

3.3. A refined bonding model for coronene

The circular shape of B_{36} (**I**) cluster and its π bonding pattern are reminiscent of coronene ($C_{24}H_{12}$), the latter containing C–C bonds for *hub*, *rim*, *flank*, and *spoke*. Such an analogy was first recognized by Chen et al.^[18] Indeed, both B_{36} (**I**) and $C_{24}H_{12}$ possess 108 electrons. Their π CMOs amount to 12 for both species, showing one-to-one correspondence (Figure 2). Being described via some 20 resonance structures or by three mobile Clar sextets, coronene itself is of

interest in chemical bonding and aromaticity.^[53–55] Boldyrev and coworkers^[53,54] recently proposed a bonding model on the basis of AdNDP analysis, which features six 2c-2e C–C π bonds on the rim, three 6c-2e π bonds on the C_6 hub, and three 24c-2e π bonds on all C centers. Kumar et al.^[55] subsequently conducted a comparative study between the Clar sextet model and the AdNDP model.

The Boldyrev model, as appealing as it looks, has certain aspects that need refinement. We shall do a CMO analysis on coronene, because CMOs are fundamental in chemical bonding. The π framework is presented in Figure 2b, whose 12 CMOs show close correspondence to B_{36} (I) cluster. Thus, in light of the comprehensive analysis presented above for B_{36} (I), the bonding in coronene is relatively easy to understand. Briefly, coronene also possesses concentric double π aromaticity, with 6π and 18π electrons for the hub and rim/flank, respectively. This overall picture is born out from our AdNDP analysis (Figure 3b; see also Figure S3). Here the inner 6π subsystem is primarily situated on the C_6 hub, which can be slightly expanded to the spokes (Figure 3b, second row). Specifically, the hub contributes to ONs by 1.67–1.87 $|e|$; that is, 84–94%. The outer 18π subsystem is completely delocalized on the C_{18} ring (rim and flank) (Figure 3b, third and fourth rows), which is intrinsically aromatic and should not be localized or segmented. As an independent support, we also performed nucleus-independent chemical shift (NICS)^[56] calculations. The NICS(1) values at PBE0 level, calculated at 1 Å above the hole center, is –5.00 ppm for coronene, as compared to –10.38 ppm for benzene. For artificially flattened D_{6h} B_{36} bowl cluster, NICS(1) amounts to –15.98 ppm. These values are all negative, in line with π aromaticity in the systems. In the Boldyrev model, the outer 18π subsystem of coronene is segmented into six 2c-2e π bonds with remaining three π CMOs being treated as global 24c-2e π bonds. Note that these 24c-2e π bonds have 3 or 4 nodal planes. This is against the building principle for an aromatic system, which requires that the bottom bond to be completely bonding (and normally with zero nodal plane).

To our personal understanding, the Boldyrev model as illustrated^[53] should imply that the rim C–C links in coronene possess a *formal* bond order of slightly greater than 2: one 2c-2e σ

bond, one $2c-2e$ π bond, plus extra contribution from three “global” $24c-2e$ π bonds. Note that a C–C bond in hydrocarbons, if indeed $2c-2e$ in nature, is anticipated to have a nearly ideal bond order of one. However, our calculated WBI values for these C–C links are only 1.58 at PBE0/6-311+G(d) level. For a calibration, benzene has a calculated WBI of 1.44, compared to a formal value of 1.50. To further ensure this, we also calculated WBIs at the B3LYP/6-311+G(d) level, and the values are 1.57 for coronene and 1.44 for benzene. In short, the PBE0 and B3LYP data are highly consistent, pointing to the fact that the actual bond order for the C–C rim in coronene appears to be far lower than that illustrated in the Boldyrev model, which is a con for the latter. Bond distances give a similar picture^[57] In contrast, the current model (Figure 5b) is consistent with all data and represents a refinement of the Boldyrev model.

As commented by one reviewer, chemical bonding model for coronene is not trivial in principle and cannot be described by only one model. This fact is nicely exemplified by numerous models created by a number of groups worldwide. This reviewer specifically stated that our current bonding model (Figure 5b) is no exception, which opinion we fully respect. Nonetheless, we would like to offer a little more details on how our model interprets the uneven C–C bonds in the outer C_{18} ring in coronene. The primary reason is that coronene has an overall D_{6h} symmetry only (rather than 9- or 18-fold symmetry, such as D_{18h}), owing to its inner C_6 core. The C centers in outer C_{18} ring are split into two types: twelve for rim versus six for flank. As a consequence, the 18 C–C links in the outer C_{18} ring are not equivalent and do not participate completely equally in π delocalization, resulting in slightly uneven WBI values (1.58 for rim and 1.27 for flank at PBE0). However, such unevenness is relatively moderate (as compared to the “double” versus “single” bonds in the Boldyrev model).^[53] Note that WBI for flank C–C bond is markedly greater than one and that for rim C–C bond markedly smaller than two, which effectively smooths the difference between the “double” and “single” C–C bonds, consistent with the outer 18π delocalization in our bonding model. We thus conclude that the uneven C–C distances in outer C_{18} ring in coronene are not a con for our updated bonding model. On the contrary, the quantitative WBI data fully support our model.

We can construct a model $C_{18}H_{18}$ monocyclic ring cluster, which indeed has D_{18h} symmetry upon optimization at the PBE0/6-311+G(d) level. Its nine π CMOs (Figure S4) show exact one-to-one correspondence to those of coronene or B_{36} (**I**) cluster, further supporting the idea that the latter two species have an outer 18π -electron aromatic subsystem (rather than 6π). The D_{18h} $C_{18}H_{18}$ cluster has uniform WBI of 1.40 for all C–C bonds, which lies in between those of rim (1.58) and flank (1.27) in coronene, because the model $C_{18}H_{18}$ cluster has an ideally delocalized 18π system (as compared to the less-than-ideal outer 18π subsystem for coronene owing to its lower D_{6h} symmetry; see above). For B_{36} (**I**), the B–B distance in the third ring (B_{18}) is also split between the 12 apex B–B links and 6 edge ones. However, this does not contradict with the outer 18π aromatic subsystem.^[58,59]

3.4. Why the hexagonal hole in B_{36} cluster prefers to be in the central position?

Liu et al.^[19] recently observed that isomers **I–III** of B_{36} cluster successively gain stability as the hexagonal hole moves from the second B ring to the first and eventually to bowl center (see Figure 1). These authors made an effort to rationalize this trend via AdNDP analysis. Nonetheless, the bonding pictures for isomers **II** and **III** did not seem to be correct due to the complex nature of the systems. Thus we believe that Liu et al. did not succeed in answering the question why the hexagonal hole in B_{36} cluster prefers to be in the central position.

We redid chemical bonding analyses for isomers **II** and **III**, via CMOs and AdNDP. The σ framework appears to be easy with the aid of AdNDP, resulting in $2c-2e/3c-2e$ ^[45] and island $4c-2e$ σ bonds that almost uniformly cover the whole surface (Figure 6). The above AdNDP data are similar to those of Liu et al.^[19] with minor discrepancies, which are not crucial. For the π framework, our key observation from CMOs is that the two spatially separated π subsystems (6π versus 18π) persist in **II** and **III**. Remarkably, the center of the π subsystems is fixed at the cluster center and does not migrate with the hexagonal hole. As an example, the complete set of π CMOs of isomer **III** are presented in Figure 4, which show correspondence to isomer **I** (Figure 2a). The AdNDP π schemes of **II** and **III** are illustrated in Figure 6. As is clearly revealed here,

the π patterns in **I–III** are largely the same, for both CMOs (Figures 4 and S2) and AdNDP schemes.^[60] Note that all ON values in AdNDP are reasonable, except for one 29c-2e π bond in **III** (1.47 |e|; Figure 6b). The latter is due to participation of the core in this specific bond, which can be traced back to the HOMO (Figure 4). Expansion of this bond to 36c-2e fully recovers ON value to 2.00 |e| (Figure S5).

The similarity of π bonding patterns in isomers **I–III** is not sufficient enough to differentiate the three isomers for energetics, despite efforts by Liu and coworkers^[19] (Figure S6b). To rationalize the trend in energetics (Figure 1), it is crucial to examine how a hexagonal hole affects orbital energies for different isomers. A few examples are shown in Figure 7 for isomers **I** and **III**, which have the largest difference in energetics. For isomer **I**, HOMO–30, HOMO–5, HOMO–17, and HOMO–3 are chosen; their corresponding CMOs in isomer **III** are HOMO–49, HOMO–16, HOMO–24, and HOMO–3, respectively.

The CMOs of **I** and **III** in left two columns in Figure 7 have major contributions from the inner core, which occurs as hexagonal B_6 ring in **I** (with a prototypical hexagonal hole) versus filled hexagonal B_7 disk in **III** (with elimination of hexagonal hole). Energetically, HOMO–30 (σ) in **I** has an orbital energy that is 3.52 eV less stable than its counterpart in **III**, despite that the former looks more symmetric and more delocalized. Similarly, HOMO–5 (π) in **I** is 1.44 eV less stable than its counterpart in **III**. This effect is unexpected and seems odd, but it is completely understandable. Here the hexagonal hole of **I** is not important, nor is its high symmetry. It is the spatial position of electron clouds, as well as the spatial match/mismatch between hexagonal hole and electron clouds, that matter. Hexagonal hole is in fact a con for a CMO that positions on it, whereas a filled hexagon hardens the disk and stabilizes a CMO, either π or σ .

Likewise, HOMO–17 and HOMO–3 in **I**, for example, are primarily located on the outer BDR ribbon with little electron cloud on central hexagon hole. In these cases, the central hexagon hole does not quite affect these CMOs. On the contrary, the migration of hexagonal hole to outer BDR ribbon in **III** effectively destabilizes their corresponding CMOs (HOMO–24 and HOMO–3), which cover the new hexagon hole. Specifically, HOMO–24 is destabilized by

0.31 eV with respect to isomer **I** and HOMO–3 by 0.44 eV. Since there are substantially more CMOs around the outer BDR ribbon in B_{36} cluster than at the vicinity of bowl center (approximately 39 versus 15 for isomer **I**; see Figure 3a), it is better to situate the hexagonal hole at bowl center. This sort of arrangement destabilizes far fewer σ/π CMOs, effectively making isomer **I** of B_{36} cluster more stable than its rivals.

4. Conclusions

Bowl-shaped B_{36} cluster is an interesting molecular model for low-dimensional boron-based nanosystems such as borophenes. We report on a revised chemical bonding model for B_{36} cluster on the basis of canonical molecular orbital (CMO) analysis and adaptive natural density partitioning (AdNDP). The cluster features concentric double π aromaticity with spatially independent inner 6π and outer 18π subsystems, each following the $(4n + 2)$ Hückel rule. This bonding picture differs than prior works on the system. We also show that the electron clouds of concentric 6π and 18π system are spatially fixed, irrespective of the migration of hexagonal hole. The latter is revealed as a destabilization factor for σ/π CMOs that cloud on it. The preference of hexagonal hole in central location in B_{36} cluster lies in the fact that substantially fewer CMOs are present around the bowl center, thus resulting in much less collective destabilization. In other words, it is minimizing destabilization from the hexagonal hole (rather than maximizing stability) that governs the global minimum of bowl-like C_{6v} B_{36} cluster.

Acknowledgements

This work was supported by the National Natural Science Foundation of China (21573138) and the Sanjin Scholar Distinguished Professors Program.

References

-
- [1] L. Hanley, J. L. Whitten, S. L. Anderson, *J. Phys. Chem.* **1988**, 92, 5803–5812.

-
- [2] E. Oger, N. R. M. Crawford, R. Kelting, P. Weis, M. M. Kappes, R. Ahlrichs, *Angew. Chem. Int. Ed.* **2007**, *46*, 8503–8506.
- [3] I. Boustani, *Int. J. Quant. Chem.* **1994**, *52*, 1081–1111.
- [4] J. E. Fowler, J. M. Ugalde, *J. Phys. Chem. A* **2000**, *104*, 397–403.
- [5] J. I. Aihara, *J. Phys. Chem. A* **2001**, *105*, 5486–5489.
- [6] J. I. Aihara, H. Kanno, T. Ishida, *J. Am. Chem. Soc.* **2005**, *127*, 13324–13330.
- [7] H. J. Zhai, A. N. Alexandrova, K. A. Birch, A. I. Boldyrev, L. S. Wang, *Angew. Chem. Int. Ed.* **2003**, *42*, 6004–6008.
- [8] H. J. Zhai, B. Kiran, J. Li, L. S. Wang, *Nat. Mater.* **2003**, *2*, 827–833.
- [9] A. N. Alexandrova, A. I. Boldyrev, H. J. Zhai, L. S. Wang, *Coord. Chem. Rev.* **2006**, *250*, 2811–2866.
- [10] Y. J. Wang, X. Y. Zhao, Q. Chen, H. J. Zhai, S. D. Li, *Nanoscale* **2015**, *7*, 16054–16060.
- [11] Y. J. Wang, J. C. Guo, H. J. Zhai, *Nanoscale* **2017**, *9*, 9310–9316.
- [12] A. P. Sergeeva, D. Y. Zubarev, H. J. Zhai, A. I. Boldyrev, L. S. Wang, *J. Am. Chem. Soc.* **2008**, *130*, 7244–7246.
- [13] W. Huang, A. P. Sergeeva, H. J. Zhai, B. B. Averkiev, L. S. Wang, A. I. Boldyrev, *Nat. Chem.* **2010**, *2*, 202–206.
- [14] B. Kiran, S. Bulusu, H. J. Zhai, S. Yoo, X. C. Zeng, L. S. Wang, *Proc. Natl. Acad. Sci. USA.* **2005**, *102*, 961–964.
- [15] Y. J. Wang, Y. F. Zhao, W. L. Li, T. Jian, Q. Chen, X. R. You, T. Ou, X. Y. Zhao, H. J. Zhai, S. D. Li, J. Li, L. S. Wang, *J. Chem. Phys.* **2016**, *144*, 064307.
- [16] W. L. Li, Q. Chen, W. J. Tian, H. Bai, Y. F. Zhao, H. S. Hu, J. Li, H. J. Zhai, S. D. Li, L. S. Wang, *J. Am. Chem. Soc.* **2014**, *136*, 12257–12260.
- [17] Z. A. Piazza, H. S. Hu, W. L. Li, Y. F. Zhao, J. Li, L. S. Wang, *Nat. Commun.* **2014**, *5*, 3113.
- [18] Q. Chen, G. F. Wei, W. J. Tian, H. Bai, Z. P. Liu, H. J. Zhai, S. D. Li, *Phys. Chem. Chem. Phys.* **2014**, *16*, 18282–18287.

- [19] L. Liu, E. Osorio, T. Heine, *Chem. Asian J.* **2016**, *11*, 3220–3224.
- [20] Q. Chen, W. L. Li, Y. F. Zhao, S. Y. Zhang, H. S. Hu, H. Bai, H. R. Li, W. J. Tian, H. G. Lu, H. J. Zhai, S. D. Li, J. Li, L. S. Wang, *ACS Nano* **2015**, *9*, 754–760.
- [21] H. J. Zhai, Y. F. Zhao, W. L. Li, Q. Chen, H. Bai, H. S. Hu, Z. A. Piazza, W. J. Tian, H. G. Lu, Y. B. Wu, Y. W. Mu, G. F. Wei, Z. P. Liu, J. Li, S. D. Li, L. S. Wang, *Nat. Chem.* **2014**, *6*, 727–731.
- [22] S. Jalife, L. Liu, S. Pan, J. L. Cabellos, E. Osorio, C. Lu, T. Heine, K. J. Donald, G. Merino, *Nanoscale* **2016**, *8*, 17639–17644.
- [23] X. B. Yang, Y. Ding, J. Ni, *Phys. Rev. B* **2008**, *77*, 041402.
- [24] X. Wu, J. Dai, Y. Zhao, A. Zhuo, J. Yang, X. C. Zeng, *ACS Nano* **2012**, *6*, 7443–7453.
- [25] Z. Zhang, Y. Yang, G. Gao, B. I. Yakobson, *Angew. Chem. Int. Ed.* **2015**, *54*, 13022–13026.
- [26] A. J. Mannix, X. F. Zhou, B. Kiraly, J. D. Wood, D. Alducin, B. D. Myers, X. L. Liu, B. L. Fisher, U. Santiago, J. R. Guest, M. J. Yacaman, A. Ponce, A. R. Oganov, M. C. Hersam, N. P. Guisinger, *Science* **2015**, *350*, 1513–1516.
- [27] B. J. Feng, J. Zhang, Q. Zhong, W. B. Li, S. Li, H. Li, P. Cheng, S. Meng, L. Chen, K. H. Wu, *Nat. Chem.* **2016**, *8*, 563–568.
- [28] Q. Zhong, L. J. Kong, J. Gou, W. B. Li, S. X. Sheng, S. Yang, P. Cheng, H. Li, K. H. Wu, L. Chen, *Phys. Rev. Mat.* **2017**, *1*, 021001.
- [29] H. S. Liu, J. F. Gao, J. J. Zhao, *Sci. Rep.* **2013**, *3*, 3238.
- [30] A. P. Sergeeva, I. A. Popov, Z. A. Piazza, W. L. Li, C. Romanescu, L. S. Wang, A. I. Boldyrev, *Acc. Chem. Res.* **2014**, *47*, 1349–1358.
- [31] D. Y. Zubarev, A. I. Boldyrev, *Phys. Chem. Chem. Phys.* **2008**, *10*, 5207–5217.
- [32] E. D. Glendening, C. R. Landis, F. Weinhold, *J. Comput. Chem.* **2013**, *34*, 1429–1437.
- [33] T. Lu, F. W. Chen, *J. Comput. Chem.* **2012**, *33*, 580–592.
- [34] C. Adamo, V. Barone, *J. Chem. Phys.* **1999**, *110*, 6158–6170.
- [35] R. Krishnan, J. S. Binkley, R. Seeger, J. A. Pople, *J. Chem. Phys.* **1980**, *72*, 650–654.

- [36] M. J. Frisch, G. W. Trucks, H. B. Schlegel, G. E. Scuseria, M. A. Robb, J. R. Cheeseman, G. Scalmani, V. Barone, B. Mennucci, G. A. Petersson, H. Nakatsuji, M. Caricato, X. Li, H. P. Hratchian, A. F. Izmaylov, J. Bloino, G. Zheng, J. L. Sonnenberg, M. Hada, M. Ehara, K. Toyota, R. Fukuda, J. Hasegawa, M. Ishida, T. Nakajima, Y. Honda, O. Kitao, H. Nakai, T. Vreven, J. A. Montgomery, Jr., J. E. Peralta, F. Ogliaro, M. Bearpark, J. J. Heyd, E. Brothers, K. N. Kudin, V. N. Staroverov, R. Kobayashi, J. Normand, K. Raghavachari, A. Rendell, J. C. Burant, S. S. Iyengar, J. Tomasi, M. Cossi, N. Rega, J. M. Millam, M. J. Klene, E. Knox, J. B. Cross, V. Bakken, C. Adamo, J. Jaramillo, R. Gomperts, R. E. Stratmann, O. Yazyev, A. J. Austin, R. Cammi, C. Pomelli, J. W. Ochterski, R. L. Martin, K. Morokuma, V. G. Zakrzewski, G. A. Voth, P. Salvador, J. J. Dannenberg, S. Dapprich, A. D. Daniels, Ö. Farkas, J. B. Foresman, J. V. Ortiz, J. Cioslowski, D. J. Fox, Gaussian 09, Revision D.01, Gaussian, Inc., Wallingford CT, **2009**.
- [37] U. Varetto, Molekel 5.4.0.8, Swiss National Supercomputing Center, Manno (Switzerland), **2009**.
- [38] R. Dennington, T. Keith, J. Millam, GaussView, version 5.0.9, Semichem, Inc., Shawnee Mission, KS, **2009**.
- [39] I. A. Popov, Z. A. Piazza, W. L. Li, L. S. Wang, A. I. Boldyrev, *J. Chem. Phys.* **2013**, *139*, 144307.
- [40] Z. A. Piazza, I. A. Popov, W. L. Li, R. Pal, X. C. Zeng, A. I. Boldyrev, L. S. Wang, *J. Chem. Phys.* **2014**, *141*, 034303.
- [41] D. Y. Zubarev, A. I. Boldyrev, *J. Comput. Chem.* **2007**, *28*, 251–268.
- [42] A. P. Sergeeva, B. B. Averkiev, A. I. Boldyrev, *Struct. Bond.* **2010**, *136*, 275–306.
- [43] The lowest-energy CMO in each set is completely delocalized and completely bonding, which is occupied first. Higher CMOs appear in pairs (normally degenerate), except for the highest energy one for even n .
- [44] I. A. Popov, A. I. Boldyrev, Classical and multicenter bonding in boron: Two faces of boron. in *Boron. The Fifth Element* (Eds: D. Hnyk, M. L. Mckee), Springer, Switzerland, 2015, pp. 1–16.

- [45] Owing to coordination environments, Lewis 2c-2e σ bonds in the first B ring and at edge positions in the third B ring can be slightly expanded to 3c-2e σ bonds. However, these 3c-2e σ bonds are predominantly contributed by two B atoms. We consider such 2c-2e/3c-2e σ bonds to be of no fundamental difference.
- [46] For these eighteen CMOs, six correspond to edge B–B σ bonds (that is, tetracoordinate sites), which appear as a regular set with from 0 to 3 nodal planes. Two B–B σ bonds associated to an apex site combine constructively or destructively to generate a pair of “local” orbitals, each type of which further combines through all apex sites to form a set of six CMOs. These twelve CMOs collectively recover twelve 2c-2e σ bonds around the apex sites in the third B ring.
- [47] J. O. C. Jiménez-Halla, R. Islas, T. Heine, G. Merino, *Angew. Chem. Int. Ed.* **2010**, *49*, 5668–5671.
- [48] G. Martínez-Guajardo, A. P. Sergeeva, A. I. Boldyrev, T. Heine, J. M. Ugalde, G. Merino, *Chem. Comm.* **2011**, *47*, 6242–6244.
- [49] D. Moreno, S. Pan, L. L. Zeonjuk, R. Islas, E. Osorio, G. Martínez-Guajardo, P. K. Chattaraj, T. Heine, G. Merino, *Chem. Commun.* **2014**, *50*, 8140–8143.
- [50] H. J. Zhai, Q. Chen, H. Bai, S. D. Li, L. S. Wang, *Acc. Chem. Res.* **2014**, *47*, 2435–2445.
- [51] H. Bai, Q. Chen, C. Q. Miao, Y. W. Mu, Y. B. Wu, H. G. Lu, H. J. Zhai, S. D. Li, *Phys. Chem. Chem. Phys.* **2013**, *15*, 18872–18880.
- [52] H. J. Zhai, Q. Chen, H. Bai, H. G. Lu, W. L. Li, S. D. Li, L. S. Wang, *J. Chem. Phys.* **2013**, *139*, 174301.
- [53] D. Y. Zubarev, A. I. Boldyrev, *J. Org. Chem.* **2008**, *73*, 9251–9258.
- [54] I. A. Popov, A. I. Boldyrev, *Eur. J. Org. Chem.* **2012**, *18*, 3485–3491.
- [55] A. Kumar, M. Duran, M. Solà *J. Comput. Chem.* **2017**, *38*, 1606–1611.
- [56] P. v. R. Schleyer, C. Maerker, A. Dransfeld, H. Jiao, N. J. R. v. E. Hommes, *J. Am. Chem. Soc.* **1996**, *118*, 6317–6318.
- [57] The C–C bond distances in coronene correlate roughly with their WBI values. At PBE0, the C–C

distances of the outer C_{18} ring in coronene are 1.37 (for rim) and 1.42 Å (for flank), respectively, and that in $D_{18h} C_{18}H_{18}$ model cluster is 1.42 Å. These three values correspond to the calculated WBIs of 1.58, 1.27, and 1.40, respectively. We believe that, in this case, WBI is a slightly better indicator for C–C bonding. For comparison, typical C–C, benzene, and C=C bonds are 1.54, 1.40, and 1.34 Å, respectively. Clearly, the rim and flank C–C bonds in coronene are in the vicinity of benzene (and $D_{18h} C_{18}H_{18}$) in terms of either bond orders or bond distances. For example, the rim and flank C–C distances are within ± 0.03 Å of benzene. In particular, the flank C–C bonds are not single bonds. All the above data concertedly point to an delocalized outer π subsystem in coronene, which largely smears the “C=C” versus “C–C” bonds in the Boldyrev model.^[53]

[58] As reasoned throughout this paper, there is no doubt that the outer BDR ribbon in B_{36} (**I**) cluster supports a 18π aromatic subsystem. This is particularly convincing in light of a close comparison with the model $C_{18}H_8$ cluster (Figure S4). We shall offer here an argument for the unevenness of apex versus edge B–B links in the third B ring in B_{36} (**I**). Two type of B centers are present in the third B ring (tricoordinate apex sites versus tetracoordinate edge sites). Their distinct coordinate environments are the primary reason for the unevenness in B–B distances, which differ in σ bonding. For the σ framework, an apex B–B link is associated to both $2c-2e$ σ and island $4c-2e$ σ bonds, whereas an edge B–B link is bound by a $2c-2e$ σ bond only^[45] (Figure 3a, first row). In other words, an apex B–B link is two-fold σ bound and an edge link is one-fold σ bound. Therefore, the unevenness of B–B distances in the third ring is not a con for the outer 18π aromatic subsystem in B_{36} (**I**).

[59] Furthermore, the outer BDR ribbon in B_{36} (**I**) does not have 9- or 18-fold symmetry due to the C_{6v} structure of the cluster, nor does the outer ribbon contain 18 rhombic B_4 units (Figure 1a). In this case, each B_4 rhombus, B_3 triangle, or B–B link can contribute differently to the outer 18π aromatic subsystem. However, such unevenness is not a con to the 18π aromaticity. This argument is in the spirit of that for coronene; see Section 3.3.

[60] Again, Liu et al.^[19] relied on the AdNDP program to produce π schemes for isomers **II** and **III**.

In their schemes, the inner 6π subsystem is destroyed and occurs randomly in space, which are inconsistent with CMOs. Note that even the number of inner π bonds can be varied in AdNDP, an example^[19] of which is shown in Figure S6b.

FIGURE CAPTIONS

- Figure 1.** Optimized bowl-shaped isomers **I–III** of B_{36} cluster at the PBE0/6-311+G(d) level. (a) Global-minimum (GM) structure **I** (C_{6v} , 1A_1). It consists of concentric $B_6/B_{12}/B_{18}$ rings from the inner core to outer periphery, defined as the *first*, *second*, and *third* boron ring, respectively. (b) Local minimum (LM) **II** (C_s , $^1A'$). (c) LM **III** (C_s , $^1A'$). Relative energies are shown in kcal mol $^{-1}$ for isomers **II** and **III**, for which the hexagonal hole is located at the first and second B ring, respectively.
- Figure 2.** Pictures of π canonical molecular orbitals (CMOs) of (a) GM **I** (C_{6v} , 1A_1) of B_{36} cluster and (b) coronene $C_{24}H_{12}$ (D_{6h} , 1A_1).
- Figure 3.** Bonding patterns based on adaptive natural density partitioning (AdNDP) for (a) B_{36} **I** (C_{6v} , 1A_1) and (b) $C_{24}H_{12}$ (D_{6h} , 1A_1). Occupation numbers (ONs) are indicated. The π clouds in **I** are spatially splitted into two regimes: an *inner* boron double ring (BDR) ribbon made of the first and second B rings versus an *outer* BDR ribbon made of the second and third B rings. In (a), six 2c-2e σ bonds in the middle of the edges (with ONs of 1.71 |e|) can be expanded as 3c-2e bonds, but that does not make a marked difference except for slightly larger ONs of 1.95 |e|. The third B center contributes 12% only.
- Figure 4.** Pictures of π CMOs of artificially flattened C_{2v} B_{36} associated to LM **III**.
- Figure 5.** Concentric double π aromaticity as revealed from the CMO and AdNDP analyses for (a) B_{36} **I** (C_{6v} , 1A_1) and (b) $C_{24}H_{12}$ (D_{6h} , 1A_1). The inner 6π and outer 18π electron-counting in bowl-like B_{36} cluster is established here for the first time, whereas the bonding model for $C_{24}H_{12}$ also differs from the literature.^[53,54]
- Figure 6.** AdNDP bonding patterns of LM structures **II** and **III** of B_{36} cluster. The ONs are indicated. The concentric double π aromatic subsystems are essentially the same as those of GM **I**, irrespective of the position of hexagonal hole.
- Figure 7.** Central hexagon hole in GM **I** of B_{36} cluster is (a) a penalty for certain CMOs such

as HOMO–30 (σ) and HOMO–5 (π), with respect to their corresponding CMOs in isomer **III** (shown in bottom panels). For other CMOs such as in (b), the hexagonal hole in GM **I** serves as a relative stabilizer. All CMO energies are given in eV.

Figure 1.

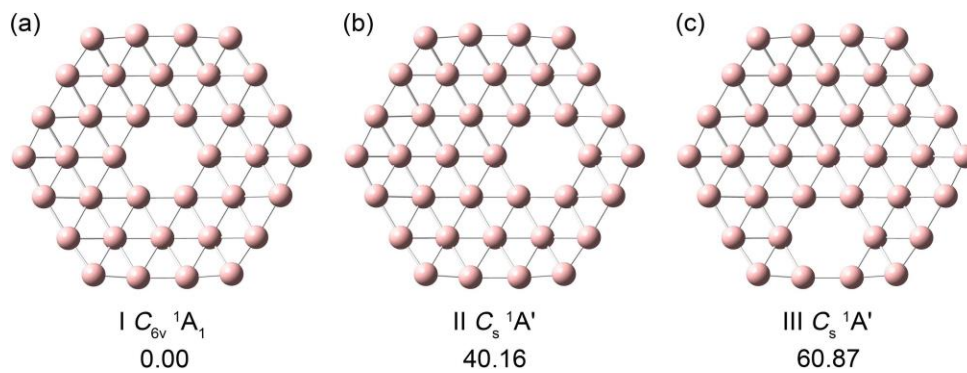


Figure 2.

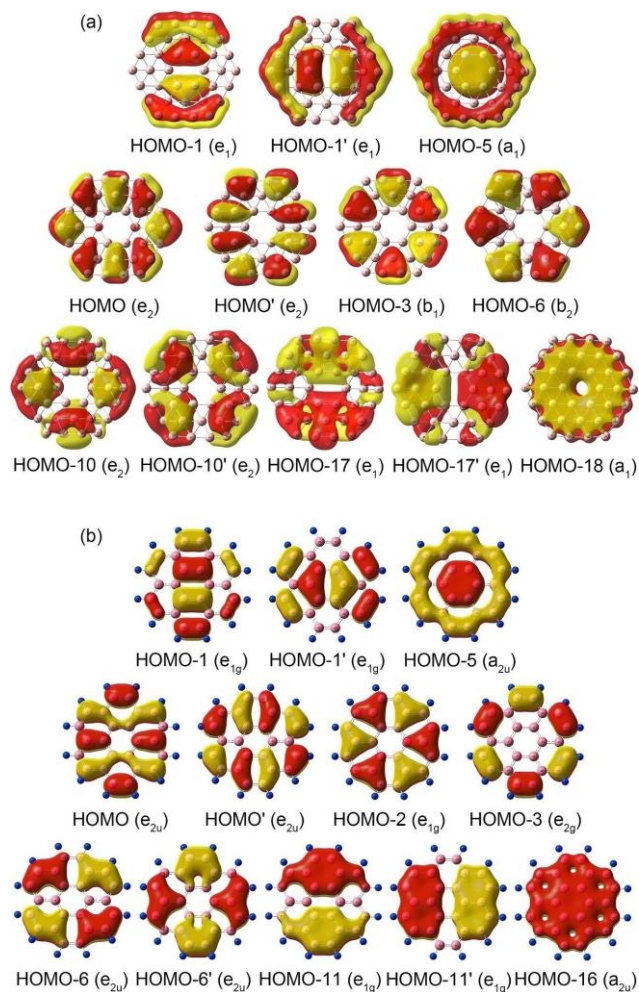


Figure 3.

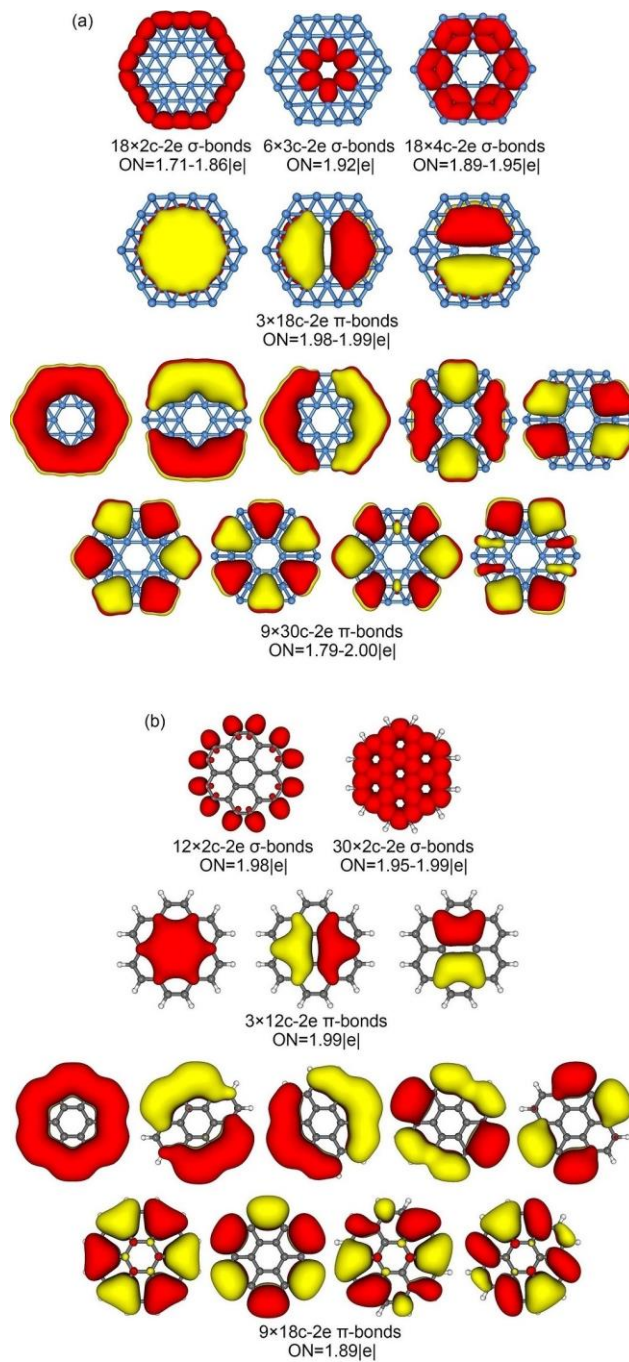


Figure 4.

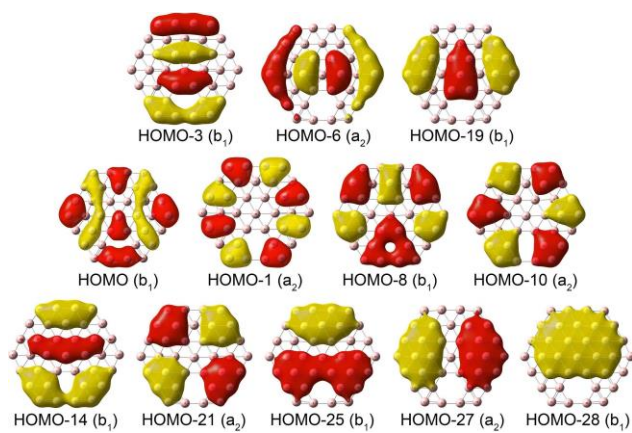


Figure 5.

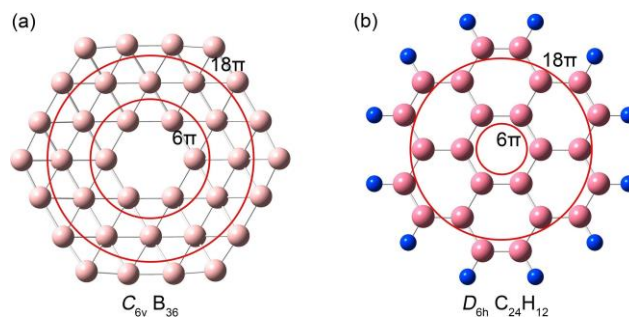


Figure 6.

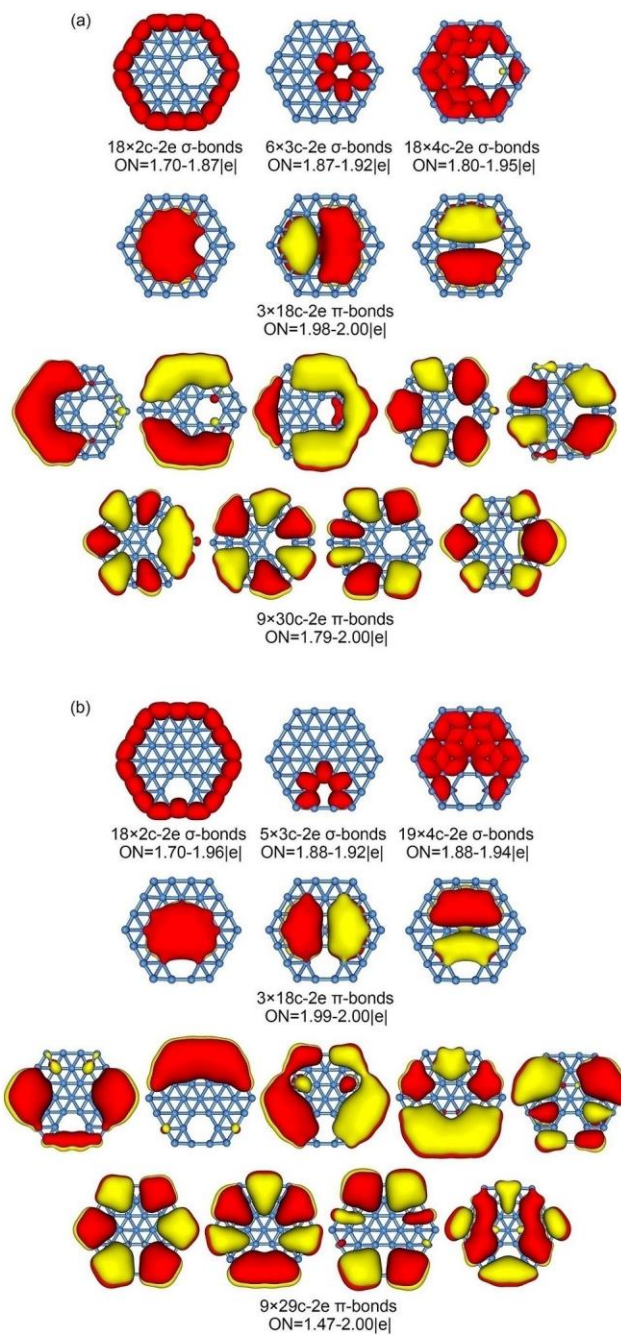


Figure 7.

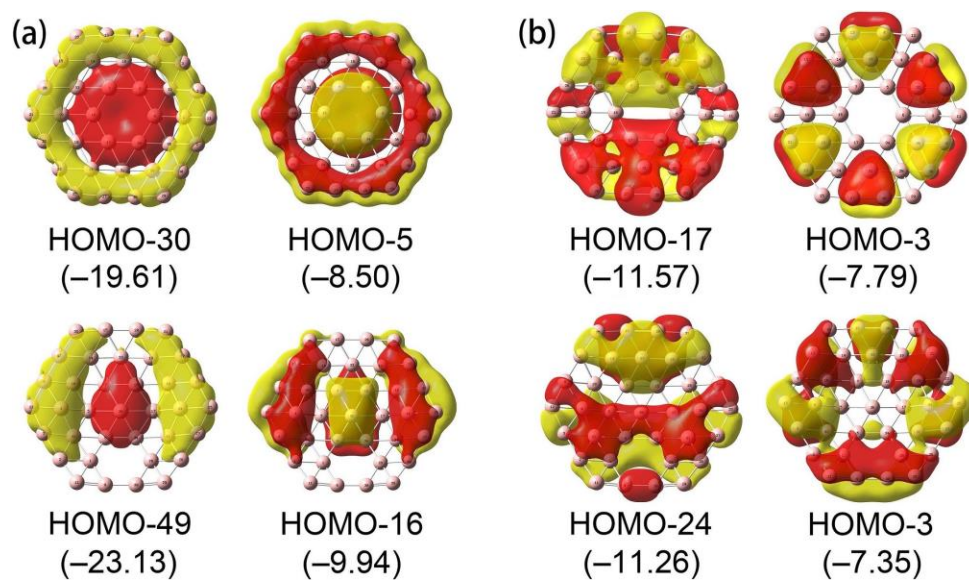
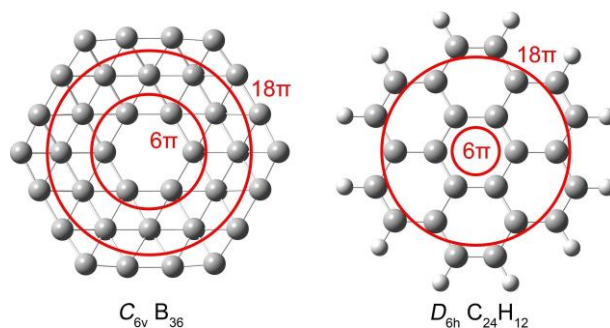


Table of Contents:



Concentric double π aromaticity. Bowl-shaped $C_{6v} B_{36}$ cluster is shown to possess inner 6π and outer 18π aromatic subsystems. This bonding pattern is retained and spatially fixed, irrespective of the migration of hexagonal hole. Our analysis also sheds crucial light on the reason why hexagonal hole in B_{36} prefers to be positioned in the bowl center.